Catalysis Today 166 (2011) 111–115

Contents lists available at ScienceDirect

Catalysis Today

journal homepage: www.elsevier.com/locate/cattod

Pt and Ni supported catalysts on SBA-15 and SBA-16 for the synthesis of biodiesel

A.E. Barrón Cruz[a,*], J.A. Melo Banda[a], Hernández Mendoza[a], C.E. Ramos-Galvan[a], M.A. Meraz Melo[c], Domínguez Esquivel[b]

[a] Instituto Tecnológico de Ciudad Madero, División de Estudios de Posgrado e Investigación, Juventino Rosas y Jesús Urueta S/N, C. P. 89440, Col. Los Mangos, Cd. Madero, Tam., Mexico
[b] Instituto Mexicano del Petróleo, Programa de Ingeniería Molecular, Eje central L. Cárdenas No. 152, México D.F., Mexico
[c] Instituto Tecnológico de Iztapalapa-III, Av. Cuitlahuac, Col. Los Reyes Culhuacan, Del. Iztapalapa, México D.F., Mexico

ARTICLE INFO

Article history:
Available online 5 February 2011

Keywords:
Biodiesel
Transesterification
Vegetable oil
Nickel
Platinum
SBA-15
SBA-16
Acid catalysis

ABSTRACT

Biodiesel is synthesized via the transesterification of lipid feedstocks with low molecular weight alcohols. Industrially, alkaline bases such as sodium and potassium hydroxides (NaOH–KOH) are used to catalyze the reaction. These catalysts require anhydrous conditions and feedstocks with low levels of free fatty acids (FFAs). Water in the reaction promotes the formation of FFAs, which can deactivate the catalyst and produce soap, an undesirable byproduct. Strong liquid acids are less sensitive to FFAs and can simultaneously conduct esterification and transesterification reactions. Solid catalysts based on Ni and Pt supported on mesoporous materials (SBA-15 and SBA-16) were tested in the synthesis of biodiesel by transesterification of a vegetable oil via acid catalysis. Textural and structural proprieties of the catalysts were characterized by N_2 physisorption (BET method), X-ray diffraction (XRD), and Transmission electron microscopy (TEM); the textural properties and XRD results showed the characteristic properties of mesoporous materials. The Cetane Index of the biodiesel obtained was tested and compared against the Cetane Index of conventional petroleum-based diesel. ASTM techniques used as comparison analysis for the synthetic biodiesel showed better properties than conventional diesel.

1. Introduction

Biomass has enough potential as a resource to produce various useful chemicals and fuels [1,2]. Biodiesel consists of alkyl esters derived from either the transesterification of triglycerides (TGs) or the esterification of free fatty acids (FFAs) with low molecular weight alcohols. The combustion of biodiesel is similar to petroleum-based diesel; thus, it can be used either as a substitute for fossil fuel or, more commonly, in fuel blends [3]. Some of its properties are biodegradability, biological origin, biorenewable nature, very low sulfur content and toxicity, low volatility/flammability, good transport and storage properties, higher cetane number, and its salutary atmospheric CO_2 balance for production; thus, it is recommended by the European Union and classified as a future fuel [4,5]. Table 1 shows a brief comparison of the ASTM standards for diesel and biodiesel. Biodiesel is comparable to traditional diesel fuel. Table 2 summarizes the typical emission profiles of biodiesel and one of its blends, B20, which consists of 20% biodiesel and 80% petroleum diesel. The table shows how biodiesel reduces noxious emissions compared to diesel, even when used as the minor component of a fuel blend. It was previously mentioned that biodiesel is commonly prepared from TG sources such as vegetable oils, animal fats, and waste greases. Oils and fats belong to an ample family of chemicals (lipids). Typically, fats come from an animal source and oils from a plant source. Fats and oils are primarily formed from a triester of glycerol (a triol) and three fatty acids. Thus, the chemical transformation of lipid feedstocks to biodiesel involves the transesterification of these TGs with alcohols to alkyl esters, as shown in Fig. 1 [6,7].

The conversion of plant oils to biodiesel has included the use of homogeneous strong base catalysts such as alkaline metal hydroxides, alkoxides, and acids such as HCl and H_2SO_4 as catalysts [8]. Alkaline alkoxides and hydroxides are considerably more effective catalysts than acid catalysts and operate at lower temperatures. Industrially, NaOH and KOH are preferred due to their wide availability and low cost; however, plant oils with high free fatty acid contents (FFAs) produce soap in the presence of homogeneous alkaline catalysts, leading to a products loss, problems with product separation, and many purification processes [6–9]. Thus, the alcohol as well as the catalysts must be essentially anhydrous (total

* Corresponding author. Tel.: +52 35748 20x3111; fax: +52 833 2158544.
E-mail address: melobanda@yahoo.com.mx (J.A. Melo Banda).

0920-5861/$ – see front matter © 2011 Elsevier B.V. All rights reserved.
doi:10.1016/j.cattod.2011.01.008

Table 1
ASTM standards for diesel and biodiesel [4,5].

Property	Diesel	Biodiesel
Standard test	ASTM D957	ASTM D6751
Composition	HC[a] (C10–C21)	FAME[b] (C12–C22)
Kin. viscosity (mm^2/s) at 40 °C	1.9–4.1	1.9–6.0
Specific gravity (g/ml)	0.85	0.88
Flash point (°C)	60–80	100–170
Cloud point (°C)	−15 to 5	−3 to 12
Pour point (°C)	−35 to −15	−15 to 16
Water (vol%)	0.05	0.05
Carbon (wt%)	87	77
Hydrogen (wt%)	13	12
Oxygen (wt%)	0	11
Sulfur (wt%)	0.05	0.05
Cetane index	40–55	48–60
HFRR[c] (μm)	685	314
BOCLE[d] scuff (g)	3600	>7000

[a] Hydrocarbons.
[b] Fatty acid methyl esters.
[c] High-frequency reciprocating rig.
[d] Ball-on cylinder lubricity evaluator.

Table 2
Average B100 and B20 emissions (in %) vs. normal diesel [8].

Emissions	B100	B20
Carbon monoxide	−48	−12
Total unburned hydrocarbons	−67	−20
Particulate matter	−47	−12
Nitrogen oxides	+10	+2
Sulfates	−100	−20
Air toxics	−60 to −90	−12 to −20
Mutagenicity	−80 to −90	−20

water must be 0.1–0.3 wt% or less). The presence of water in the feedstock promotes hydrolysis of the alkyl esters to FFAs (Fig. 2(a)). Because of the soap formation in the alkaline transesterification process (Fig. 2(b)), the total FFA content associated with the lipid feedstock must not exceed 0.5 wt% [10]. In order to conform to these demanding feedstock specifications, it is necessary to use highly refined vegetable oils whose price can account for 60–75% of the final cost of biodiesel [11]. The homogeneous acid-catalyzed reaction is slower than the homogeneous base-catalyzed reaction [12]. However, the acid-catalyzed transesterification process is not strongly affected by the presence of FFAs in the feedstock. In fact, acid catalysts can simultaneously catalyze both esterification and transesterification reactions. Thus, the advantage of acid catalysts is biodiesel production from low-cost lipid feedstocks, (FFAs levels of ≥6%). Acid-catalyzed production of biodiesel can compete with a base-catalyzed process using virgin oils, especially when the former uses low-cost feedstocks [13,14]. Usually, sulfuric acid (H_2SO_4) is used as a catalyst in homogeneous acid-catalyzed reactions, which, although effective, lead to serious contamination problems, which translate into higher production costs. Additionally, some characteristics are necessary: for example, a continuous process and fewer reaction steps, a limiting number of separation processes, and use of a heterogeneous catalyst, which can be incorporated into a packed bed continuous flow reactor, simplifying product separation and purification [6].

2. Experimental

2.1. Synthesis of catalysts

Mesoporous supports SBA-15 and SBA-16 were prepared using a triblock polymer, poly(ethyleneoxide)-poly(propyleneoxide)-poly(ethyleneoxide) (EO-PO-EO) as the structure directing agent, and tetraethyl orthosilicate (TEOS) as the silica source. In a typical synthesis, 4 g of Pluronic P123 for SBA-15 and 2 g of Pluronic F127 for SBA-16 were each dispersed in 150 ml and 80 ml of 0.5 M HCl solution, respectively. For SBA-16, 14.1 g of NaCl were added. Finally, 9 g of TEOS for SBA-15 and 8.4 g for SBA-16 were added to each homogeneous solution with stirring to form a reactive gel. The mixtures were stirred at 318 K for 24 h. Then, the reaction mixture was submitted to hydrothermal treatment (aging) at 363 K for 24 h. The resulting solids were isolated by filtration, washed with deionized water and dried at 353 K for 12 h. For SBA-16, removal of the F127 template was carried out by solvent extraction using ethanol and HCl. SBA-15 and SBA-16 were both calcined in air at

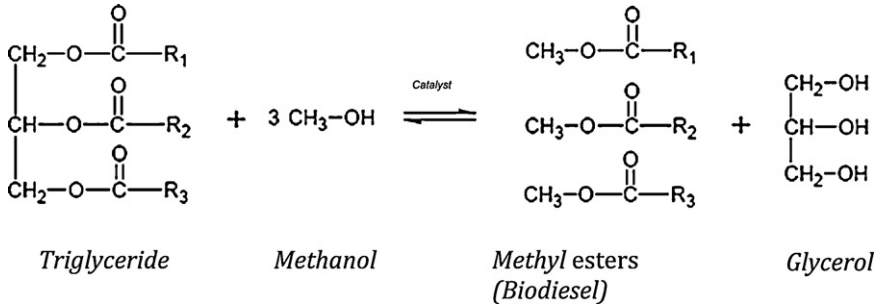

Fig. 1. Typical trans-estherification reaction of a triglyceride with methanol [8].

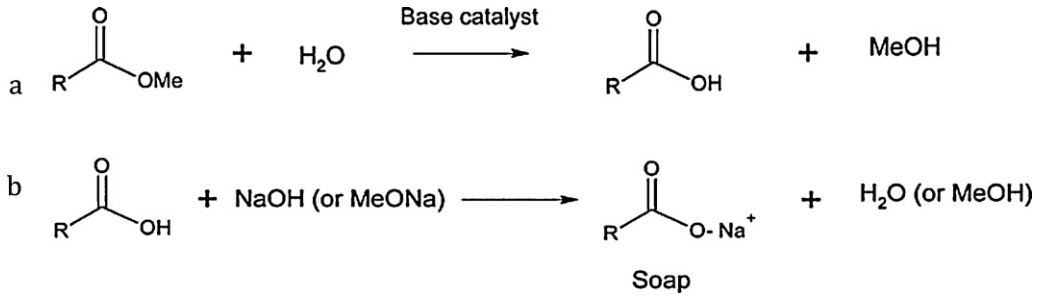

Fig. 2. (a) Water promotion of FFA's. (b) FFA's reaction with basic catalysts to produce soap and water (i.e., undesirable byproducts).

Table 3
Fatty acid composition of canola oil.

Acidity index	Composition (wt%)
Palmitic (C16:0)[a]	4
Stearic (C18:0)	2
Oleic (C18:1)	62
Linoleic (C18:2)	22
Linolenic (C18)	10

[a] Numbers in parenthesis means the number of carbon atoms and double bonds.

823 K for 6 h, with a slow temperature increase [15,16]. The support materials were incipient wetness impregnated with aqueous solutions of nickel nitrate ($Ni(NO_3)_2{\cdot}6H_2O$) and platinum(II) acetylacetonate ($Pt(C_5H_7O_2)_2$) to load 2.5, 5, and 10 wt% for SBA-15Ni and SBA-16Ni, and 2.5wt% for SBA-15Pt and SBA-16Pt, respectively. After drying at 373 °C for 2 h, the catalysts were calcined at 823 K for 6 h in air. The names for the prepared catalysts can be found in Table 3.

2.2. Characterization of the catalysts

Textural properties of the catalysts were characterized by N_2 physisorption (BET method) using a Quantachrome Autosorb-1 apparatus. Structural arrangement of the materials was determined by X-ray diffraction (XRD) using a Difractometer BRUKER AXS D8 ADVANCE with a Cu Kα X-ray source. Transmission electron microscopy (TEM) images were collected on an FEI Tecnai G^2 30 microscope operated at 300 kV.

2.3. Reaction test

A 1000 ml stirred glass reactor was used for the transesterification of canola oil to biodiesel. Eighty milliliters of canola oil and 20 ml of methanol (molar ratio of methanol to canola oil 6:1) were added into the reactor with 1 g of catalyst, and then the temperature was raised to 333 K under stirring for 4 h. The biodiesel was isolated by decantation in a separating funnel, allowing the glycerol to separate from the methyl ester by gravity for 3 h. The biodiesel yield was calculated from the methyl ester and vegetable oil weights. Two homogeneous catalyzed reactions using NaOH and H_2SO_4 were carried out in order to compare the yields with heterogeneous catalyzed reactions. The molecular weight of canola oil was calculated according to the compositions of fatty acids shown in Table 4 [17]. The physical properties and chemical composition of biodiesel were tested according to the ASTM D975 test method.

Table 4
Textural properties of supports and catalysts.

Material	S_A (m^2/s)	V_P (cc/g)	[a]D_p (Å)	Metal (wt%)
SBA-15	890	0.98	44	–
SBA-15Ni 2.5	753	0.71	38	2.5
SBA-15Ni 5	693	0.40	34	5
SBA-15Ni 10	403	0.28	35	10
SBA-15Pt 2.5	733	0.75	36	2.5
SBA-16	934	0.63	27	–
SBA-16Ni 2.5	345	0.30	35	2.5
SBA-16Ni 5	209	0.28	33	5
SBA-16Ni 10	199	0.26	35	10
SBA-16Pt 2.5	294	0.26	33	2.5

Surface area (S_A), pore diameter (D_p) and pore volume (V_P).
[a] Pore diameter determined from desorption isotherm by the BJH method.

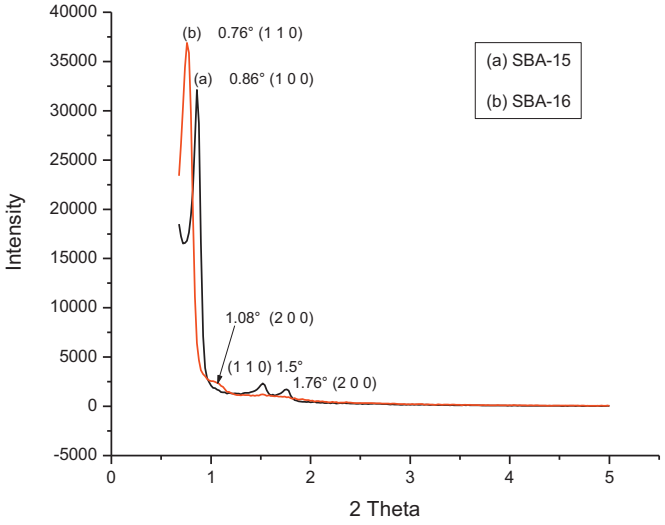

Fig. 3. XRD patterns of mesoporous supports: (a) SBA-15 and (b) SBA-16.

3. Results and discussion

3.1. Structural properties

The total surface areas, the pore volumes, and the pore size of the supports and catalysts were calculated from the N_2 adsorption–desorption isotherms, and the results are summarized in Table 5. The total surface areas of SBA-15 and SBA-16 supports were high but decreased after metals loading. Fig. 3 shows

Table 5
Physical properties and chemical composition of biodiesel and fossil diesel.

Sample	Cetane index	Viscosity 40 °C (mm^2/seg)	Density (g/cc)	C (wt%)	H (wt%)	O (wt%)	S (wt%)
NaOH	52	4.71	0.89	75	13	12	<0.05[a]
H_2SO_4	50	4.52	0.85	78	10	9	<0.05[a]
SBA-15 Ni 2.5%	49	4.96	0.93	77	12	11	<0.05[a]
SBA-15 Ni 5%	51	4.82	0.90	75	12	12	<0.05[a]
SBA-15 Ni 10%	50	4.77	0.89	75	13	11	<0.05[a]
SBA-16 Ni 2.5%	49	4.92	0.90	78	10	8	<0.05[a]
SBA-16 Ni 5%	52	4.78	0.90	75	13	13	<0.05[a]
SBA-16 Ni 10%	51	4.65	0.88	77	13	10	<0.05[a]
SBA-15Pt 2.5	52	4.56	0.86	75	13	12	<0.05[a]
SBA-16PT 2.5	51	4.42	0.86	76	12	13	<0.05[a]
Mexican diesel[b]	48	3.0	–	–	–	–	0.03
American diesel[b]	44	2.5	–	–	–	–	0.03
European diesel[b]	50.5	2.58	–	–	–	–	0.09
Japanese diesel[b]	53.2	3.0	–	–	–	–	0.13

[a] These values correspond to the lower limit of detection from ASTM D975 test method, but it's estimated absent.
[b] These data were adopted from literature.

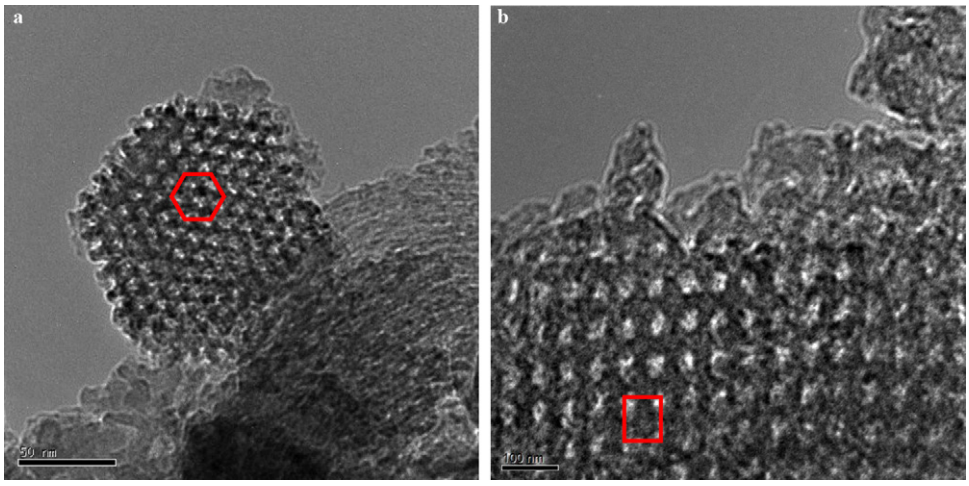

Fig. 4. TEM micrographs of the mesoporous supports showing the typical hexagonal and square pore symmetries: (a) SBA-15 and (b) SBA-16.

the N_2 adsorption–desorption isotherms for the supports SBA-15 (a), and SBA-16 (b). Fig. 3(a) shows a type IV isotherm with H1 hysteresis, which is characteristic of a mesoporous material with uniform size and shape. On the other hand, Fig. 3(b) shows a type IV isotherm with an H2 type hysteresis, which is attributed to mesoporous materials with different pore mouth size and pore body (ink-bottle shaped pores) [18]. The XRD patterns of supports are shown in Fig. 4, where the support SBA-15 (a) shows a strong reflection (i.e., $2\theta \approx 0.8^\circ$) and two small peaks around 1.6°-2θ, which are assigned to (1 0 0), (1 1 0), and (2 0 0) reflections of a 2D hexagonal structure [19]. A very strong (1 1 0) reflection ($2\theta \approx 0.74^\circ$) from a cubic structure and a small (2 0 0) reflection ($2\theta \approx 1.12^\circ$) are detected in SBA-16 (b) [20]. The hexagonal and cubic symmetries for SBA-15 and SBA-16 are confirmed in Fig. 5, where the TEM images of SBA-15 (a) and SBA-16 (b) are shown. The XRD pattern of the catalysts after calcination (Fig. 6) shows similar peaks at $2\theta = 37^\circ$, 43°, and 62°, which are characteristic of NiO (1 0 1), NiO (1 0 2), and NiO (1 1 0), respectively [21]. Platinum

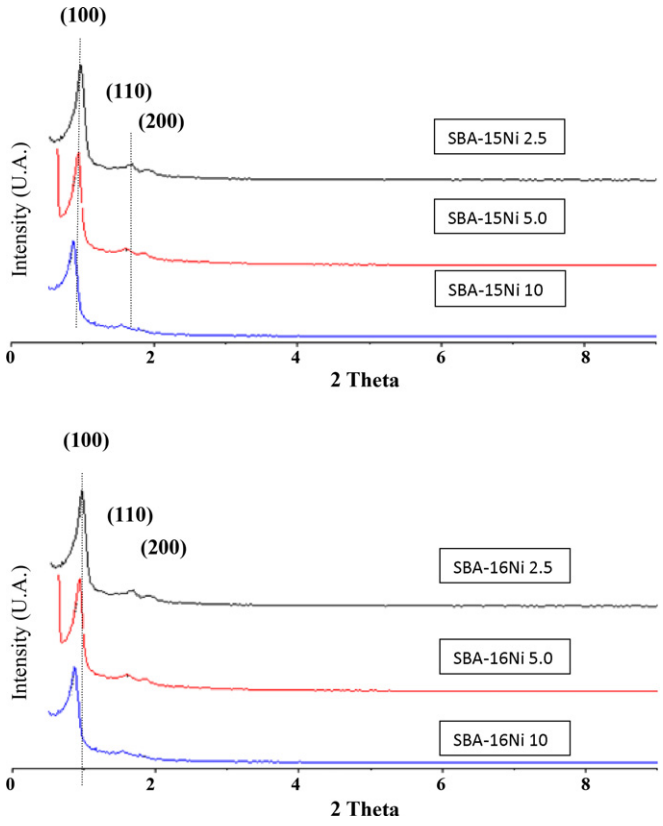

Fig. 5. Small angle XRD patterns of supported catalysts Ni/SBA-15 and SBA-16.

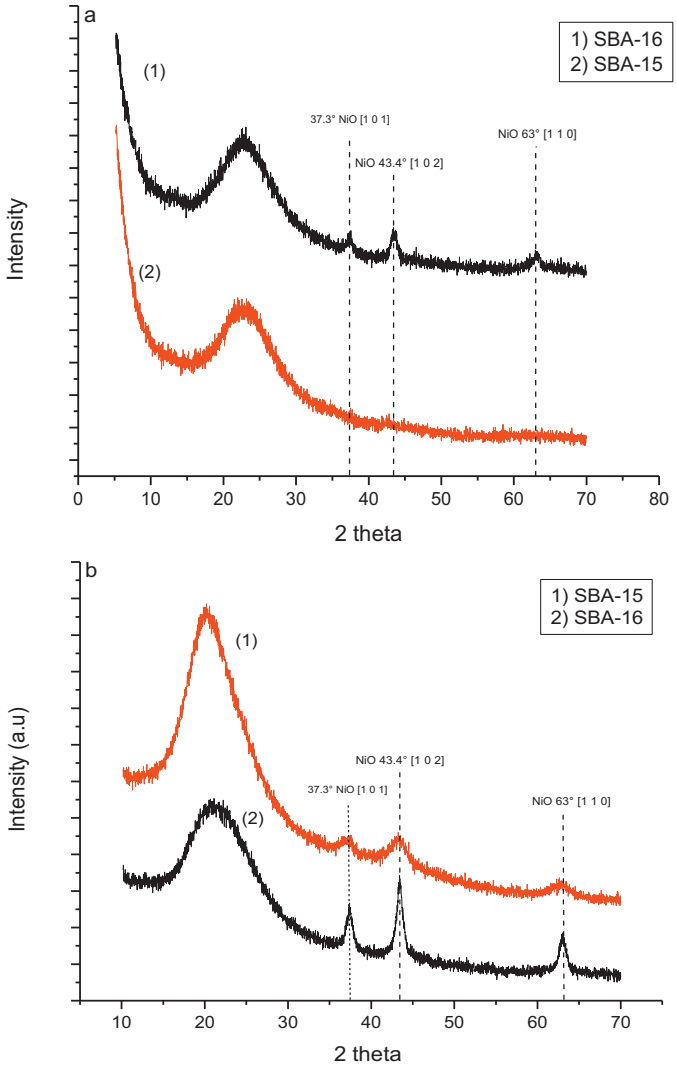

Fig. 6. XRD patterns of catalysts Ni/SBA-15 and Ni/SBA-16: (a) 5 wt% and (b) 10 wt%.

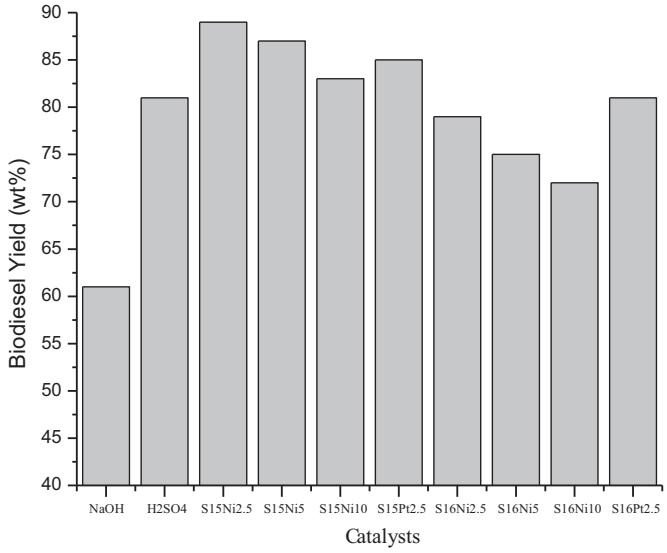

Fig. 7. Etherification reaction of canola oil to biodiesel using different acid catalyst. The Molar ratio methanol/oil was 6:1 (T = 333 K, 4 h).

supported catalysts are not shown to cause this metal a reflection peak loss. The characteristic peaks of NiO are stronger in catalysts supported on SBA-16; which means that the metal concentration in catalysts supported on SBA-16 is higher than SBA-15. This confirms the decrease of surface area of SBA-16 when metals are loaded.

The XRD patterns of the Pt and Ni/SBA (2.5 wt%) and the Ni/SBA-15 (5 wt%) catalysts did not show the characteristic peaks of PtO and NiO, respectively (see Fig. 6(a)), which could be an indication of the high dispersion of the metal phase.

3.2. Biodiesel production

The catalytic activities of the heterogeneous catalysts having different amounts of loaded metals, and homogeneous acid and basic catalysts were measured, and the biodiesel yield (wt%) as measured and presented for each catalyst all are presented in Fig. 7. The catalysts supported on SBA-15 were more active than catalysts supported on SBA-16, which could be attributed to a decrease in the surface area of the SBA-16 metals that were loading. The homogeneous basic catalyst (NaOH) showed the worst activity, with a yield of around 60 wt%. The catalyst with the best yield to produce biodiesel was SBA-15Ni 2.5% (89% of yield). All the acid catalysts had good catalytic activity with conversions above 70%, even with homogeneous acid catalysts (i.e., H_2SO_4), whose yield to biodiesel was above eighty percent. After the reaction, the biodiesel fraction was isolated by decantation, thus separating glycerol from biodiesel. After separation, the physical properties and chemical composition of biodiesel were tested according to the ASTM D975T method. Table 5 shows the results obtained in this test as well as some properties of four different conventional fossil diesels [22]. In this table, it can be observed that all samples of biodiesel synthesized via acid heterogeneous catalysis had quality properties very close to conventional fossil diesel. Also, in all cases the cetane number is bigger than that of the Mexican petroleum diesel currently used.

4. Conclusions

Nickel and platinum catalysts supported on mesoporous silica, SBA-15 and SBA-16, were successfully tested in the synthesis of biodiesel by transesterification of canola oil via acid catalysis. The textural and structural properties of the catalysts showed the characteristic properties of mesoporous materials. All the heterogeneous catalysts showed conversions above 70%. However, catalysts supported on mesoporous SBA-15 were more active than catalysts supported on SBA-16, with SBA-15Ni 2.5 wt% having the best yield of biodiesel (89% of yield). The physical properties and chemical composition of the biodiesel were better than conventional fossil diesel, which may be a viable option to compete with petroleum-based diesel as a cleaner, high quality fuel.

References

[1] L.R. Lynd, H. Jin, J.G. Michels, C.E. Wyman, Dale. Available from: http://rmtools.org/ref/Lynd_et_al_2002.pdf (June 24, 2005).
[2] A. Haryanto, F. Sandun, M. Naveen, A. Sushil, Energy Fuels 19 (5) (2005) 2098–2106.
[3] J.A. Kinast, K.S. Tyson, Production of Biodiesels from multiple stocks and properties of biodiesels and biodiesel(diesel blends, Final Report, National Renewable Energy, 2003, NREL/sr-510-31460.
[4] A.V. Tomasevic, Siler-Marinkovic, Fuel Process. Technol. 81 (2003) 1.
[5] R. Chinta, R.Venkat, O. Reed, G.V. John, Department of Chemistry, Gilman Hall, Iowa State University, February 22, 2006.
[6] L. Edgar, I. Yijun, L. Dora, S. Kaewta, G. James Jr., Ind. Eng. Chem. Res. 44 (2005) 5353–5363.
[7] C.E. Goering, A.W. Schwab, M.J. Dangherty, E.H. Pryde, A.J. Heakin, ASAE 25 (1982) 1472–1483.
[8] For reviews on transesterification of vegetable oils and animal fat to biodiesel, see:
(a) U. Schuchardt, R. Sercheli, R.M.J. Vargas, Braz. Chem. Soc. 9 (1998) 199;
(b) A.J. Kinney, T.E. Clemente, Fuel Process. Technol. 86 (2005) 1137;
(c) M.J. Haas, Fuel Process. Technol. 86 (2005) 1087;
(d) G. Knothe, Fuel Process. Technol. 86 (2005) 1059.
[9] S. Shah, S. Sharma, M.N. Gupta, Energy Fuels 18 (2004) 154.
[10] M.J. Haas, Lipid Technol. 16 (2004) 7–11.
[11] D. Talley, Render Mag. (2004) 20–21.
[12] A. Srivastava, Renew. Sustain. Energy 4 (2000) 111–133.
[13] Y. Zhang, M.A. Dube, D.D. McLean, M. Kates, Bioresour. Technol. 89 (2003) 1–16.
[14] Y. Zhang, M.A. Dube, D.D. McLean, M. Kates, Bioresour. Technol. 90 (2003) 229–240.
[15] D. Zhao, J. Feng, Q. Huo, N. Melosh, G.H. Fredrickson, B.F. Chmelka, et al., Science 279 (1998) 548–552.
[16] D. Zhao, Q. Huo, J. Feng, B.F. Chmelka, G.D. Stucky, J. Am. Chem. Soc. 120 (24) (1998) 6024–6036.
[17] Fathy acid and lipid chemistry Frank Gunstone Blackie Academic @ Profesional First Ed., 1996.
[18] G. Leofantia, M. Padovanb, G. Tozzolac, B. Venturellica, Catal. Today 41 (1998) 207–219.
[19] L. Yanga, Y. Qia, X. Yuanb, J. Shenb, J. F Kimc, J. Mol. Catal. A: Chem. 229 (2005) 199–205.
[20] C.-F. Cheng, Y.-C. Lin, H.-H. Cheng, Y.-C. Chen, Chem. Phys. Lett. 382 (2003) 496–501.
[21] Y. Park, T. Kang, J. Lee, P. Kim, H. Kim, J. Yi, Catal. Today 97 (2004) 195–203.
[22] K. Tomislav, K. Nenad, R. Damir, Rudarsko-geološko-naftni zbornik 19 (2007) 79–86.